17th World Conference on Earthquake Engineering, 17WCEE
Sendai, Japan - September 13th to 18th 2020

NON-GAUSSIAN CHRACTERISTC OF ACCELERATION TIME HISTORY

T. Sato[(1)], I. Yoshida[(2)], Y. Murono[(3)]

[(1)] *Emeritus Professor, Kyoto University, satotdnbseu@yahoo.co.jp, Honmachi Yoshida, Sakyo, Kyoto*
[(2)] *Professor, Tokyo City University, iyoshida@tcu.ac.jp, 1-28-1 Tamatutumi, Setagaya, Tokyo*
[(3)]*General Manager, Railway Technical Research Institute, murono.yoshitaka.51@rtri.or.jp, Kunitachi, Tokyo*

Abstract

The main purpose of this study is to extract the non-Gaussian characteristics of the acceleration time history of earthquake motion. Using several observed acceleration time histories discretized by an equal time interval, Δt, we discuss the stochastic characteristic of the mean gradient of acceleration time history. We find that the probability distribution characteristic of the mean gradient of acceleration is expressed by the truncated Levy-flight distribution but it shows a nonstationary feature. We, therefore, calculate the standardized mean acceleration gradient defined by the ratio between the mean acceleration gradient and average acceleration amplitude at the time interval of Δt. Assuming this is a stochastic variable we calculate the probability distribution characteristic of the standardized mean acceleration gradient and show its non-Gaussian feature. Then we search a candidate of probability density function to be able to express this non-Gaussian feature and find that the Cauchy distribution is the best fitting. To make clear the fractal feature of the acceleration time history we calculate the standardized mean gradient for a lager time interval of $k\Delta t$ ($k = 1,2,5,10,15,20$) and find that the standardized mean gradient with lager discrete time intervals coincide with the same probability density function. This means that the jerk divided by the acceleration amplitude has a fractal nature because its approximations expressed by the standardized mean gradients has the same distribution characteristic independent of discrete time intervals.

Keywords: acceleration time histry, non-Gaussian characteristic, truncated Levy-flight distribution, Cauchy distribution, stochastic process

1. Introduction

The random time series like an earthquake acceleration time history is usually analyzed by using the concept of Fourier analysis [1], in which the acceleration time history is simulated based on the invers Fourier transform using the modeled Fourier amplitude and phase [2]. Because the time history of acceleration shows a strong non-stationery characteristic the time-frequency analysis of Fourier amplitude has been developed [3]. However the modeling of the Fourier phase has not attracted people's attention and the phase has been simulated by independently and identically distributed normal distribution. Sato [4] and Abdelrahman and et. al. [5] noticed that the phase of earthquake acceleration has a correlative feature with respect to the circular frequency and proposed to use the fractional Brownian motion [6] to simulate earthquake motion phase. But Sato [7] found that the stochastic characteristic of earthquake acceleration Fourier phase had the non-Gaussian feature expressed by the Levy-flight probability density function and developed the Levy-flight stochastic process to simulate a realistic earthquake motion phase. Moreover Sato [8] also found that the stochastic characteristic of earthquake acceleration Fourier amplitude had the non-Gaussian feature expressed by the Levy-flight probability density function. Based on these results we have a confidence that even the acceleration time history itself possesses the non-Gaussian characteristic. The main purpose of this paper is to discuss the procedure to extract the non-Gaussian feature directly from the recorded acceleration time histories

2. Preprocessing of an observed earthquake time history

The used earthquake acceleration time history is the EW component recorded at MYG015 observation station during the 2011 earthquake off the Pacific coast of Tohoku. Fig.1 shows the acceleration time history $a(t)$ and the normalized power of acceleration time history $e(t)$, which is the square sum of acceleration amplitude

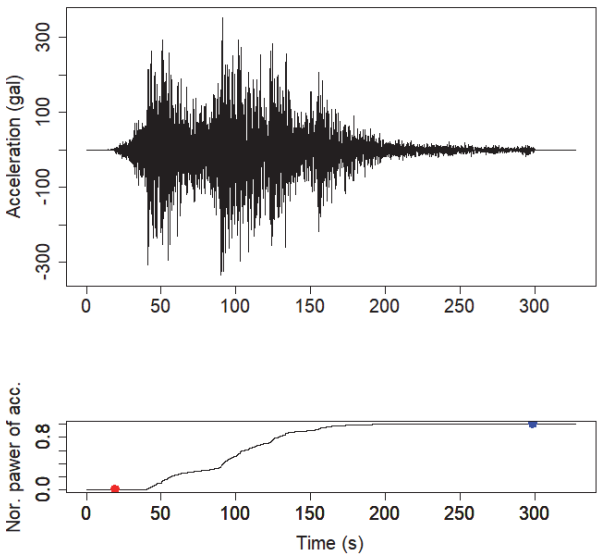

Fig.1 Upper: the used acceleration time history, Bottom: Normalized power of acceleration time history $e(t)$.
The used time band is defined by the time interval between the red and blue circles. The red circle is the point at where the normalized power $e(t)$ has the value of $\varepsilon = 0.00001$ and the blue circle is the point at where the normalized power $e(t)$ has the value of of $(1-\varepsilon)$.

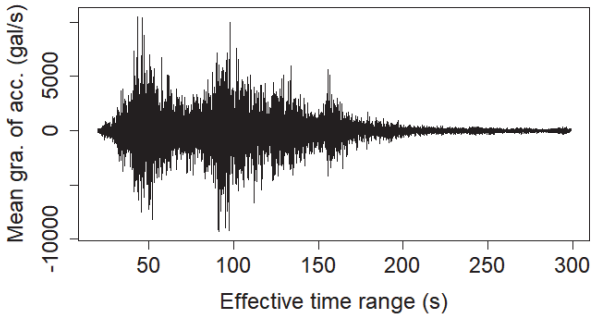

Fig.2 Time history of $\bar{J}_j$ within the time range between red and blue circls in Fig.1.

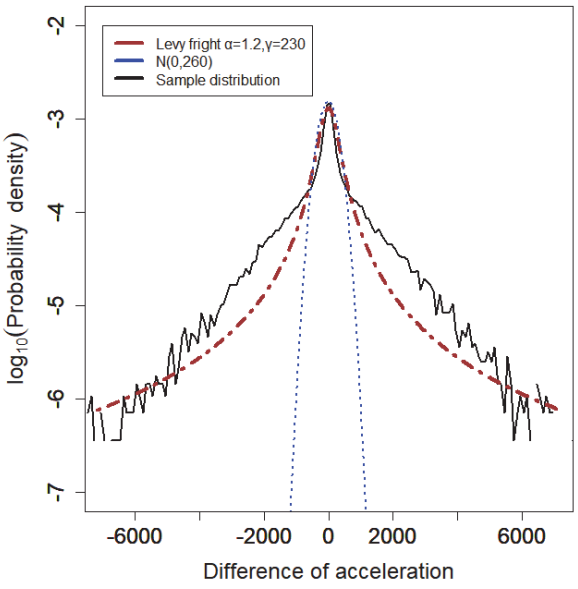

Fig.3 The probability density function of $\bar{J}_j$ shown in Fig.2.

normalized by the final value of square sum. In this paper we use the following definition of the mean gradient of acceleration, which is an approximation of the jerk.

$$\bar{J}_j = \frac{\Delta a_j}{\Delta t} = \frac{a_j - a_{j-1}}{\Delta t} \tag{1}$$

where $a_j = a(t_j)$, t_j is the discretized time expressed by $t_j = j \cdot \Delta t$, Δt is the time increment. Fig.2 is the time history of $\bar{J}_j$ within the time range between the red and blue circles shown in Fig.1. As expected the shape of time history of $\bar{J}_j$ has the same shape of acceleration time history except the amplitude becomes 100 times because of $\Delta t = 0.01s$. In Fig.3, the full black zigzag line shows the probability density function (PDF) obtained by using the data set of $\bar{J}_j$ and using the proper class width proposed by Scott [9]. For comparison two theoretical PDFs are shown in the figure. One is Levy-flight PDF [10] and the other is the Normal PDF. It is clear from this figure that the PDF of $\bar{J}_j$ has a non-Gauusian feature but cannot be expressed by Levy-flight PDF. Although there is no explicit formula of the PDF for the Levy-flight distribution the characterisitic

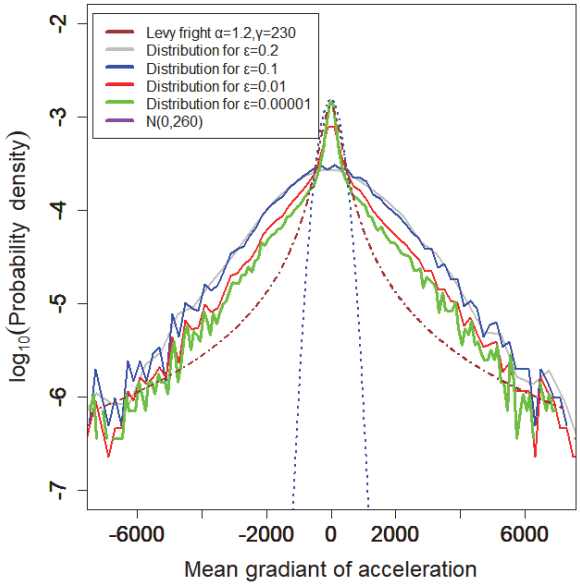

Fig.4 The PDF differences caused by the difference of time window lengths, which are controlled by ε values.

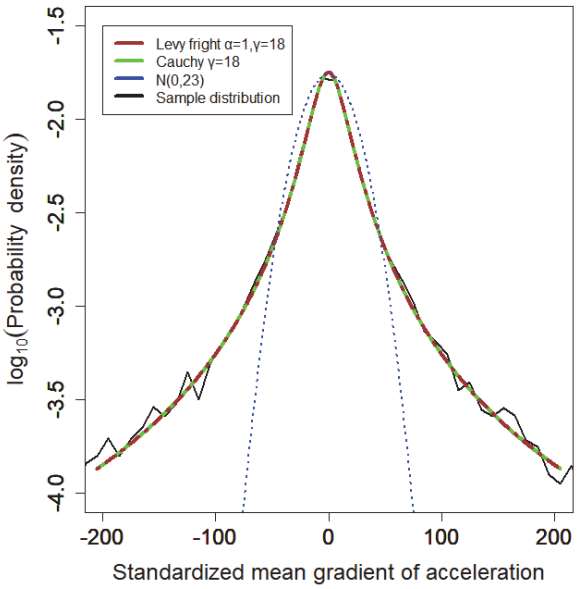

Fig.5 The PDF of B_j defined by Eq.(2), The full black zigzag line is detemined by using the recorded accleration time history. The brown chain line is the Lavey-flight PDF with $\alpha = 1$ and $\gamma = 18$. The full yellow line is the chausy PDF with $\gamma = 18$.

function of the origin symmetric Levy-flight PDF is given by using two parameters $0 < \alpha \leq 2$ and $0 < \gamma$ as follows [11]:

$$\varphi(2\pi t, \alpha, \gamma) = E[exp(-i2\pi tZ)] = exp(-\gamma^{\alpha}|2\pi t|^{\alpha}) \quad (2)$$

The Fourier inverse transform of this characteristic function gives the PDF as follows:

$$S(\alpha, \gamma, Z) = \frac{1}{2\pi}\int_{-\infty}^{\infty} \varphi(2\pi t, \alpha, \gamma) e^{i2\pi tZ} d(2\pi t) \quad (3)$$

The brown chain line in Fig.3 is the Levy-flight PDF with the characteristic parameters of $\alpha = 1.2$ and the scale parameter of $\gamma = 230$. The blue dotted line in Fig.3 is a normal PDF expresses as $N(0,260)$. Because the time history of $\bar{J}_j$ has the nonstationary feature we check this feature from the stand point of PDF. The result is shown in Fig.4. This is obtained by changing time window length of acceleration time history based on the selection of four different value of $\varepsilon = 0.2, 0.1, 0.01, 0.00001$. The peak value of PDF becomes larger as the value of ε becomes smaller.

2. Standerdized mean gradiant of acceleration

Because the nonstationary characteristic of the mean gradient of acceleration is very strong it is not so easy to grasp the whole stochastic feature of acceleration time history we, therefore, consider a new stochastic value defined by

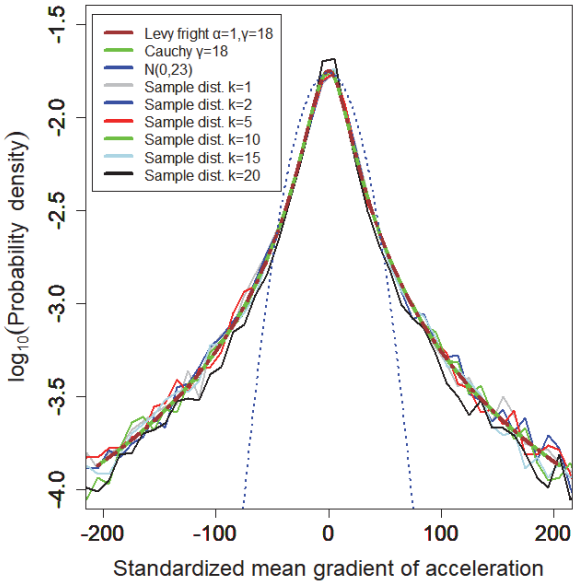

Fig.6 The fractal characteristic of B_j.

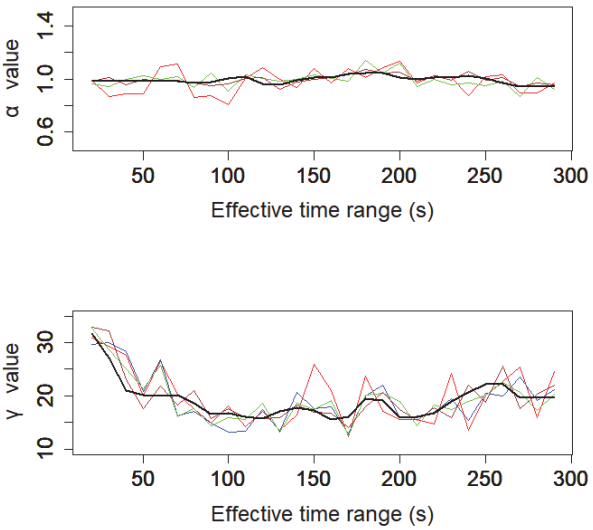

Fig.7 Nonstationary characteristics of parameters defining the Levy-flight PDF.

$$B_j = \frac{\bar{J}_j}{0.5 \cdot (a_j + a_{j-1})} = \frac{\frac{\Delta a_j}{\Delta t}}{0.5 \cdot (a_j + a_{j-1})} \tag{4}$$

At the limit of $\Delta t \to 0$ the mean gradient of accelertation $\bar{J}_j$ becomes the time history of the jark expressed by $J(t) = da(t)/dt$ then B_j becomes a time function expressed by

$$B(t) = \frac{J(t)}{a(t)} = \frac{\frac{da(t)}{dt}}{a(t)} \tag{5}$$

In Fig.5, the full black sigzag line is the PDF of B_j obtained based on Eq.(4) using a proper class width, the brown thick chain lin is the Levy-flight PDF with $\alpha = 1$ and $\gamma = 18$. The Levy-flight PDF with $\alpha = 1$ bcomes the Cauchy PDF [12] with the same γ value as defined by

$$P(B_j) = \frac{1}{\pi} \frac{\gamma}{(B_j - \delta)^2 + \gamma^2} \tag{6}$$

where δ is a location parameter. İn Fig.5, the green full line is the Cauchy PDF with $\delta = 0$ and $\gamma = 18$. The blue dotted line is the normal PDF expressed by $N(0,23)$. Both the Levy-flight PDF with $\alpha = 1$ and $\gamma = 18$ and the Cauchy PDF with $\delta = 0$ and $\gamma = 18$ are exactry overlapped. This reslts in that the PDF of the jark normalized by the accerelation amplitude fefined by Eq.(5) can be modeled by the Cauchy PDF.

3. Fractal feature hidden in the acceleration time history

Because the Fourier phase and amplitude of acceleration time history have the fractal characteristic [7,8] the acceleration time history itself should have the fractal feature. To discuss this phenomenon we define a new mean gradient of acceleration time history by.

$$\bar{J}_j(k) = \frac{\Delta a_j(k)}{k \cdot \Delta t} = \frac{a_j - a_{j-k}}{k \cdot \Delta t} \tag{7}$$

The difference between $\bar{J}_j$ defined by Eq.(1) and $\bar{J}_j(k)$ depends the difference of time intervals. In this case the standrdized mean gradient of aceeleration is defined by

$$B_j(k) = \frac{\bar{J}_j(k)}{0.5 \cdot (a_j + a_{j-k})} \tag{8}$$

In Fig.6, we show the PDF calculated from the recorded acceleration time history for different values of $k = 1,2,5,10,15,20$. These PDFs for different k are distinguished by colored lines expressed in the figure legend. It is noticed that all PDFs are almost same and coincide with the PDF of Levy-flight distribution with $\alpha = 1.0,\ \gamma = 18$ and the PDF of Cauchy distribution with $\delta = 0,\ \gamma = 18$. This means that all standardized mean gradients of acceleration coincide regardless of time interval to calculate the mean gradient of acceleration. This definitely shows that the observed acceleration time history has the fractal characteristic [13].

4. Stationary characteristic of Levy-flight probability density function

The origin symmetric Levy-flight PDF is defined by two parameters named as the characteristic index α and the scale index γ, which are identified by using the histogram of B_j and the maximum likelihood method [14] . But those parameters listed in Fig.5 are constant values. We check here this feature of parameters. The time history of B_j is divided at each 10 second and using 1, 3, 9, 15 second length of B_j data from the divided points we identified two parameters of α and γ. The result is shown in Fig.7. The difference of the time window lengths of 1, 3, 9, 15 seconds is distinguished by red, blue, brown and black lines, correspondingly. From this figure $\alpha \cong 1.0$ is confirmed. Although the parameter γ is fluctuate with time, especially it has large value at the beginning of time, the value of γ is fluctuate around $\gamma = 18$ after 50 seconds. This guarantees the result shown in Fig.5.

5. Non-Gaussian characteristic in several recorded Acceleration time history

We select the following six observed earthquake motions to confirm the non-Gaussian characteristic hidden in the recorded earthquake accelerations. They are, the NS component observed at the Kushiro Observatory during the 1993 Off-Kushiro earthquake (M=7.5), the EW component observed at Suttsu Observatory during the 1993 Off-Hokkaido south-east earthquake (M=7.8), the EW component observed at Nemuro Observatory during the 1994 Off-Hokkaido east earthquake (M=8.2), the NS component observed at Kobe Marine Meteorological Observatory during the 1995 Hyogoken-Nanbu earthquake (M=7.3), the NS component observed at K13 Observatory during the 1977 Kaogoshima north west earthquake (M=6.3) and the NS component observed at Kameoke Observatory during the 2004 Off-Kii peninsula earthquake (M=7.4).

The PDFs of the standerdaized mean gradient of acceralation obtained from these records are shown in Fig.8. Form this figure we confirm that the non-Gaussian characteristic of acceleration time history is the general feature being able to see in the observed earthquake motions.

6. Stochastic model to simulate acceleration time history

6.1 Basic consideration for modeling a stochastic differential equation

We investigate here the stochastic model to simulate the acceleration time history based on the avobe disucctions. The main purpose here is to detect a form of non-Gaussian stochastic diffrential equation from a real observed accelrartion time history. First we can rewrite Eq.(5) as the form of a stochastic differential equation as follows:

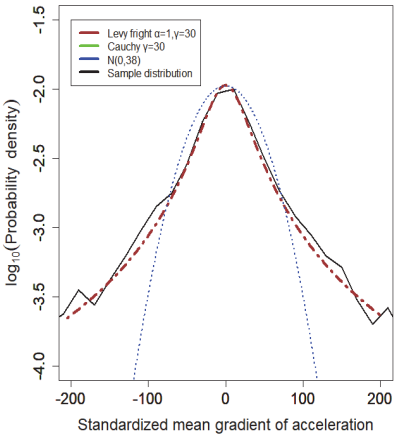

(a) Kushiro

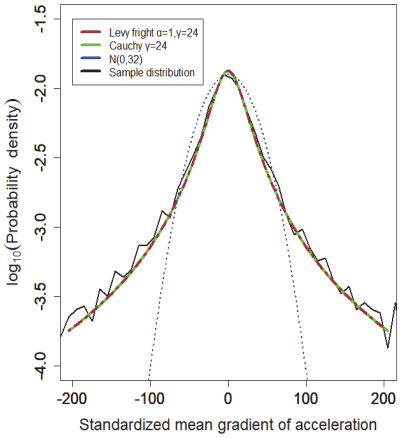

(b) Suttsu

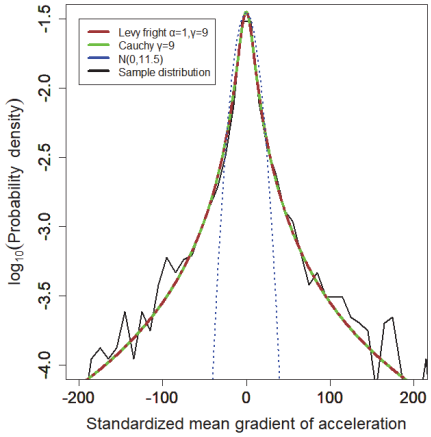

(c) Amagasaki

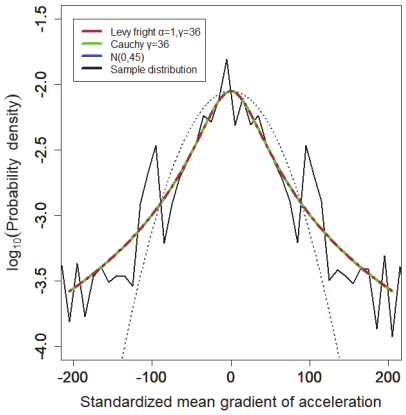

(d) Nemuro

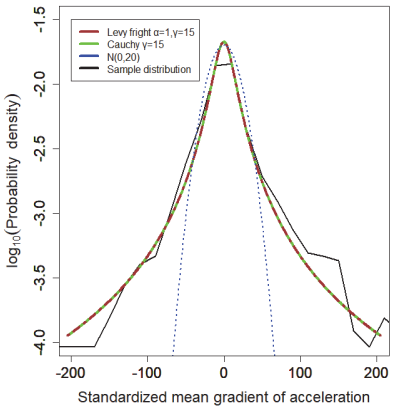

(e) Kobe

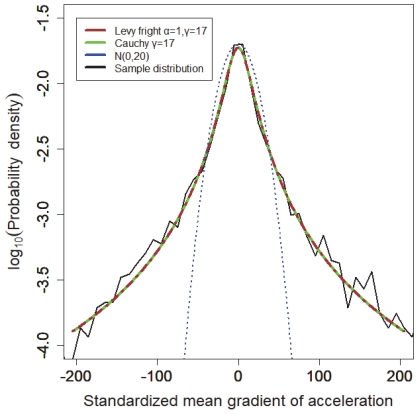

(f) Kagoshima K13

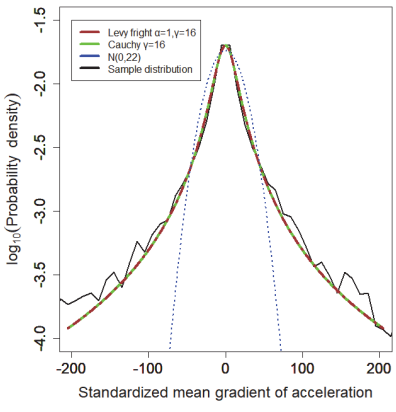

(g) Kameoka

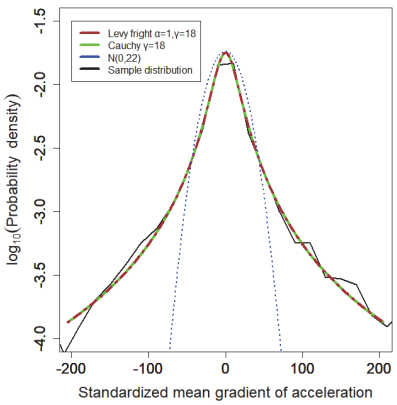

(h) MGY015 (After Shock)

Fig.8 The probability density functions for several different standardized mean gradient of accelerations.

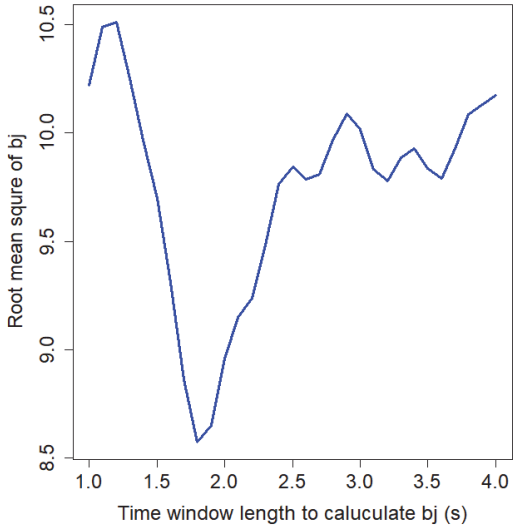

Fi.9 The relation between the length of time window and the total pwer of b_j.

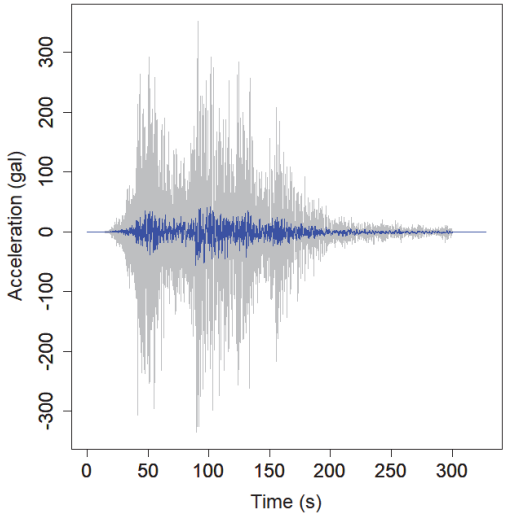

Fig.10 The base line time history of b_j (blue) and original acceleration time history (gray).

$$\frac{da(t)}{dt} = B(t)a(t) \tag{9}$$

Because this is the homogeneous defferential equation, if the $B(t)$ is time integrable the formal solution of this equation is given by

$$a(t) = Ce^{\int B(t)dt} = Ce^{\beta(t)} \tag{10}$$

where $\beta(t)$ is defined by

$$\beta(t) = \int B(t)\,dt \tag{11}$$

and C is a prameter defined by an initial condition of $a(t)$ at $t = 0$. If $\beta(0)$is exist we have $C = a(0)/e^{\beta(0)}$. Therefore we obtain $a(t) \equiv 0$ provided $a(0) \equiv 0$. Even if the $B(t)$ is a non-Gaussian stochastic process the solution of Eq.(9) is controled by the initial value expressed by $a(0)$. Therefore Eq.(9) is not proper form of a stochastic differencial equation to simulate earthquake acceleration time history, at least the driving term should be included in the stochastic differntial equation as expressed by Eq.(9).

6.2 Consideration of a driving term in the stochastic differential equation

To define the standardized mean gradient of acceleration we used the direct acceleration amplitude. In this section we use an anther measure of acceleration amplitude expressed by

$$A_j = a_j - b_j \tag{12}$$

where b_j is a sort of base line corection term defined below. Because the base line to evaluate the acceleration amplitude may fluctuate around zero acceleration line we assume that b_j is obtined by multiplying a rectangular window with proper length to the recorded acceleration time history and taking an average of acceleration within the window length. The window length is determined as the total power of b_j has minimum value. Fig.9 shows the relationship between the window length and the total power of b_j. The lowest power

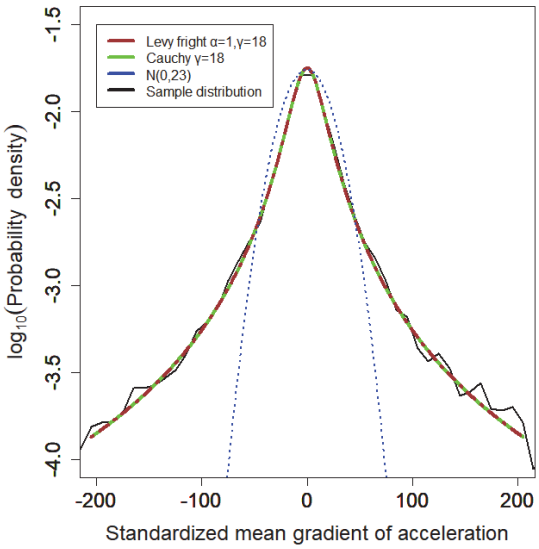

Fig.11 The PDF of B_j defined by Eq.(13).

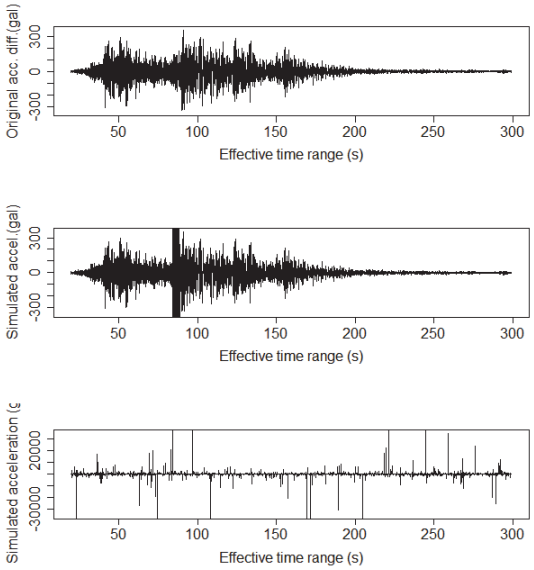

Fig.12 The acceleration time history.
Upper: Original time history,
Middle: Regenerated time history,
Bottom: Time history of B_j dfine by Eq.(13).

can be seen at the time window lenth of 1.8 seconds. Fig.10 shows the determined time history of b_j with blue line and the original acceleration time history with gray line.

Using the amplitude measure of acceleration time history defined by Eq.(12) we modify the definition of standardized mean gradient of acceleration time history as follows:

$$B_j = \frac{\bar{J}_j}{0.5 \cdot (A_j + A_{j-1})} = \frac{\frac{\Delta a_j}{\Delta t}}{0.5 \cdot (A_j + A_{j-1})} \tag{13}$$

Fig.11 shows the PDF of the new B_j. The result is almost same with the PDF shown in Fig.5 because the value of b_j is very small. Based on Eq.(13) we have the following equation at the limt of $\Delta t \to 0$

$$\frac{da(t)}{dt} = B(t)\{a(t) - b(t)\} \tag{14}$$

Comparing this equation with Eq.(9) this is a type of inhomogeneous and non-Gaussian differential equation because the $B(t)b(t)$ is an inhomogenous term.

6.3 Numerical solution of Eq.(14)

Because the integrability of Eq.(14) is not clear we use the Euler approximation [15] for numerical integration of Eq.(14). The increment of the acceleration $da(t)$ is apploximated by

$$da(t_j) \cong \Delta a_j = a_{j+1} - a_j \tag{15}$$

Substituting this formula and $B(t_j) = B_j$ as well as $a(t_j) = a_j$ and $b(t_j) = b_j$ into Eq.(14) we obtain

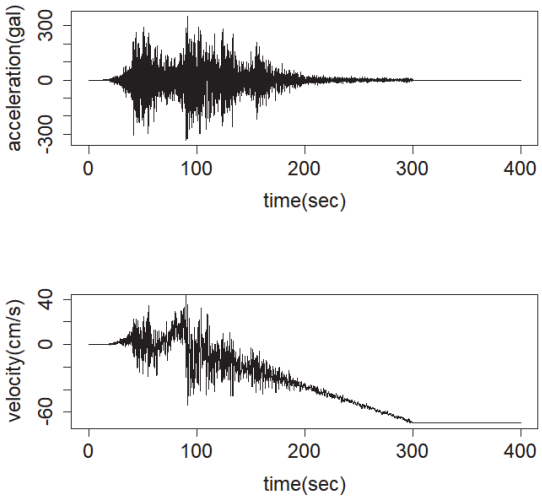

Fig.13 Acceleration and velocity time histories of observed recored at MGY015 station.

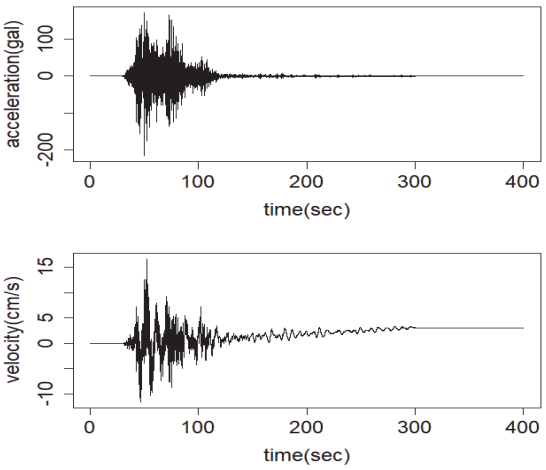

Fig.14 Aceelertaion and vlocity time history of observed recored at Suttsu station.

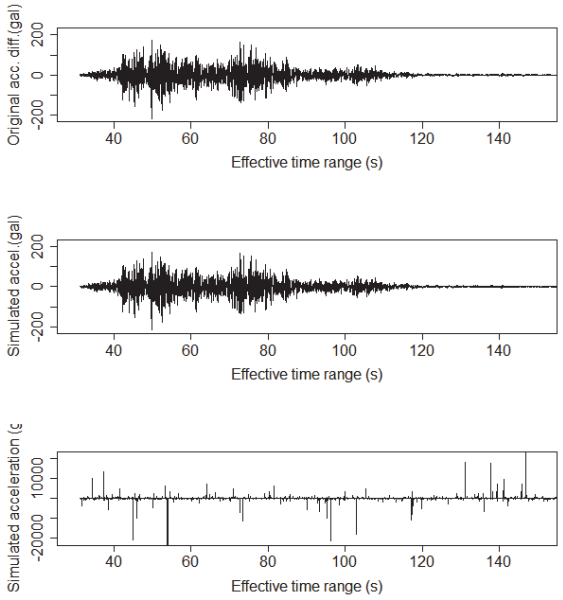

Fig.15 Observed ond simulated acceleration time history.
Upper: original,
Middle: simulated ,
Bottom: time history of B_j dfine by Eq.(13).

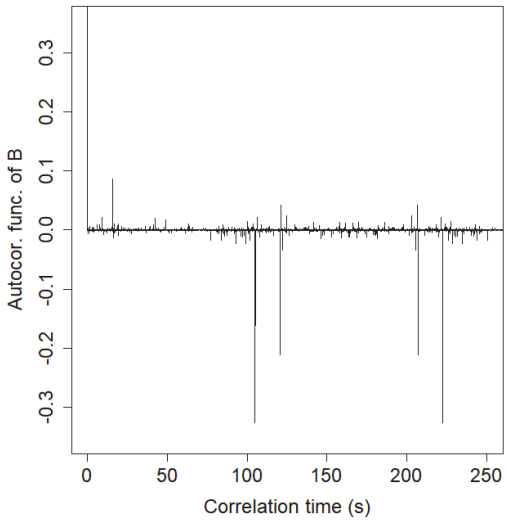

Fig.16 Auto-correlation function of B_j.

$$a_{j+1} = (1 + B_j \cdot dt)a_j - B_j \cdot dt \cdot b_j \quad (16)$$

Using this equation and B_j value obtained by Eq.(13) as well as b_j shown in Fig.10 by the blue line we resimulate the acceleration time history shown in Fig.2. The result is shown in Fig.12, in which there are three figures, the upper is the original acceleration time history, the middle is the resimulated acceleration time history and the bottom is the time history of B_j. Comparing the upper and the middle figures the configuration of resimulated acceleration time histry is compleatly different aronund time of 90s. To make clear the reason why this difference is occurred we caluclate the velocity time history. The bottom in Fig.13 shows the velocity time history obtained by integrating the acceleration. Because the base line of the velocity time histry is bended around 90s this bend causes the unexpected large amplitude of resimulated acceleration time histry. Therfore we choose the earthquake acceleration time history recorded at Suttsu Observatory of which velocity time history does not show strong bend as shown in Fig.14. Fig.15 shows the resimmulated acceleration time history based on Eq.(16) for Suttsu recored. The upper figure is the original acceleratаion time history, the middel is the resimulated one, the bottom is the time history of B_j. This shows the effectiveness of recursion formula given by Eq.(16) to resimlate the observed acceleration time history.

Then there is a possibility to simulate a acceleration time history by taking into account the uncertantiy of the concerened acceleration time history because the time history of B_j dfine by Eq.(13) is a sample of stochastic process that represents the uncertainty of the standerdized mean gradient of acceleration time history. Because the sum of random numbers generated from the Cauchy PDF under the assumption of independent and identically distributed (iid) has the reproductive property, we can assume that we can simulate the stochastic process $\{a_j\}$ by replacing B_j in Eq.(13) with the iid random numbers generated from Cauchy PDF expreed by $\{Y_j\}$. For this case, the discretized stocastic process of $a_j = a(t_j)$ can be expressed by using Euler type numerical approximation as follows:

$$a_{j+1} = (1 + Y_j \cdot dt)a_j - Y_j \cdot dt \cdot b_j \quad (17)$$

But the stochastic process a_j does not vonverge because the used dicrete time interval $dt = 0.02$s is too large and the iid asumpsion to generate Y_j is not accepted. Based on Fig.6 the standerdized mean gradiant of rcorded acceleration time history has the fractal feature, i.e. it has long memory. To make clear this phenomenon the autocorrelaton function of B_j is shown in Fig.16 for the case of recorded acceleration time history at Sutssu Observatory. Form this fiure we have to take into account at least this kind of autocorrelation feature to generate Y_j to be sued for simulating a realistic earthquake accereation time history. This is remained for a future sutudy.

7. Concluding remarks

This paper discusses the non-Gaussian feature hidden in observed earthquake acceleration time histories. The main result is that the probability density function of the jerk normalized by the acceleration amplitude is expressed by the Cauchy distribution. Based on this stochastic feature of the normalized jerk we extract a form of the stochastic differential equation with non-Gaussian feature. We also discuss the numerical approximation of the derived stochastic differential equation and reason why the numerical conversion con not be gurantteed.

8. Acknowledgements

The author would like to acknowledge the Japan Meteorological Agency and the National Research for Earth and Disaster Resilience to provide valuable observed earthquake records. We also acknowledge the supports from JSPS, Grant-in-Aid for Scientific Research #18K04334.

9. References

[1] Papoulis A 1962) *: The Fourier integral and its applications,* McGraw-Hill, New York.

[2] Priestley M B (1981): *Spectral Analysis and Time Series-PartII.* London, Academic Press.

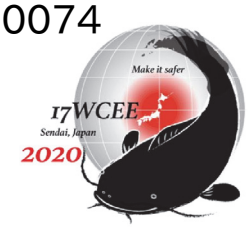

[3] Choen L (1995): *Time-Frequency Analysis*, Prentice Hall PTR, A Simon Schuster Co., New Jersey.

[4] Sato T(2013) : Fractal characteristic of phase spectrum of earthquake motion, *Journal of Earthquake and Tsunami*, 7(2), 1350010-1-17.

[5] Abdelrahman AA, Sato T, Wan C, Zhao L (2019): Simulation of Earthquake Motion Phase considering Its Fractal and Auto-covariance Features, August 2019, *KSCE Journal of Civil Engineering* **23**(11) 1-11.

[6] Mandelbrot BB, Van JW(1968) : Fractional Brownian motions, fractional noises and applications, *SIAM Review*, **10** (4), 422-437.

[7] Sato T (2018): Stochastic process of earthquake motion phase and its inherent features, *Proceedings of the 16th European conference on Earthquake Engineering*, Thessaloniki, Greece, paper No.128.

[8] Sato T(2017): Stochastic characteristics of Fourier amplitude in observed earthquake motions, *Journal of JSCE, Structural Dynamics and Earthquake Engineering,* **73**(4) I_282-I_293, (in Japanese)

[9] Scott DW (1992): *Multivariate Density Estimation, Theory, Practice and Visualization*, Wiley.

[10] Voit J (2010) : *The Statistical Mechanics of Financial Market*, Third Edition, Berlin Heidelberg, Springer-Verlag, 120-129.

[11] Nolan JP (2015, Nov.13 Browsing): http://academic2.american.edu/~jpnolan/stble/chap1. pdf, Stable Distribution, Models for Heavy Tailed Data.

[12] William F (1971). *An Introduction to Probability Theory and Its Applications, Volume II.* New York: John Wiley & Sons Inc. 2nd edition.

[13] Falconer K (2003) : *Fractal Geometry; Mathematical Foundation and Application,* 2nd ed. John Wiley & Sons, Ltd, The Atrium, Southern Gate, Chichester.

[14] R Core Team (2015): A language and environment for statistical computing. R Foundation for Statistical Computing, Vienna, Austria, URL https://www.R-project.org/, Package "libstableR" by Royula-del-Val, et.al. Ver.1.0.2, 2018-08-26.

[15] Mikosch T (1998): *Elementary Stochastic Calculus with Finance in View,* World Scientific Publishing Co. Pte. Ltd.

